Bull. Chem. Soc. Jpn., 75, 2075–2078 (2002)

# Electronic Characterization of Dimethyl 1,2-Dihydropyrrolo[1,2-*a*]quinoxaline-2,3-dicarboxylate in Solution and in the Solid State

**Keisuke Hirano, Seiji Yamaoka, Satoshi Minakata, and Mitsuo Komatsu***

Department of Applied Chemistry, Graduate School of Engineering, Osaka University,
Yamadaoka 2-1, Suita Osaka 565-0871

(Received March 29, 2002)

Dimethyl 1,2-dihydropyrrolo[1,2-*a*]quinoxaline-2,3-dicarboxylate is red colored in the solid state, while it is a small molecule and has no hydrogen-bonding interaction. This unusual color property was investigated by means of electronic characterization in solution and in the solid state. The push-pull system from electron-donating pyrrole nitrogen to the electron-withdrawing 3-methoxycarbonyl moiety causes a spectral shift to an orange color in the visible region. An X-ray structure analysis indicated that these polar molecules ($\mu = 7.6$ D) are arranged in a zig-zag fashion so as to minimize the electrostatic energy. As a consequence, the absorption band is presumably shifted toward longer wavelengths by about 60 nm (about 2508 $cm^{-1}$) in going from a solution to the solid state. These results lead to a large bathochromic shift in the absorption spectrum, resulting in the red color of this compound in the solid state.

As stated by the aromaticity rule ("Hückel's rule"), colored substances are mostly aromatic compounds of the type typically found in dyes and pigments. In order to have a red color, the organic molecules generally require long π-conjugation systems, and to have large molecular weights, such as azo dyes and perylenes.[1–4] On the other hand, quinacridones and dioxopyrrolopyrroles, which belong to the class of hydrogen-bonded materials, such as indigo analogues, are industrially important red pigments.[5–8] One of the appealing features of H-bonded pigments is their brilliant red or blue colors in the solid state, even though their molecular weights are relatively small.[9–11]

Recently, we have found a novel red colorant, dimethyl 1,2-dihydropyrrolo[1,2-*a*]quinoxaline-2,3-dicarboxylate (**1**) (Fig. 1), which has a low molecular weight (288), but does not participate in intra- or intermolecular hydrogen bonding. More interestingly, its dehydrogenated product, dimethyl pyrrolo[1,2-*a*]quinoxaline-2,3-dicarboxylate (**2**), is colorless. The deviation of the chemical structures between **1** and **2** stems from only one C–C bond in the pyrrole moiety, which is a single bond in **1** and a double bond in **2**, respectively. This indicates that **2** formally satisfies the "Hückel rule" in that it contains 14 π electrons and **1** is formally antiaromatic; however an inconsistency exists in that **2** is colorless in spite of its extensive π-conjugation. In addition to the above-mentioned rule, the contribution of a charge-transfer state based on the push-pull system also leads to color development in some compounds. In compounds **1** and **2**, the electron-donating moiety (push) is a pyrrole nitrogen and the -withdrawing one (pull) is a methoxycarbonyl group. Therefore, electronic characterizations of these compounds focusing on the electron-donating property of this nitrogen were performed in order to understand the mechanism of this large spectral shift of **1** toward a longer wavelength, as compared to **2**. In addition to the push-pull interaction, an exiton coupling effect of **1** in the solid state is also reported.

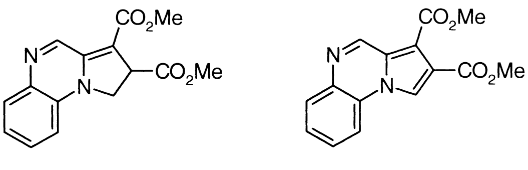
**1** **2**

Fig. 1. Chemical structures of **1** and **2**.

## Experimental

Compounds **1** and **2** were prepared by previously reported procedures with slight modifications.[12,13] Single crystals of **1** were grown by recrystallization from a hexane-dichloromethane solution. Reflection data were collected by means of a RAXIS-RAPID Imaging Plate from Rigaku Denki, and the structure was solved by a direct method (SHELXS 86).

Absorption spectra were obtained with a Hitachi U-3300 spectrometer. Polarized reflection spectra were measured on a single crystal of **1** by means of a UMSP 80 microscope-spectrophotometer (Carl Zeiss).

The geometries of molecules **1** and **2** were optimized using version 2.0 of the AM1 Hamiltonian of MOPAC.[14] Optical absorption bands were computed on the optimized geometry using the INDO/S Hamiltonian (MOS-F), and 125 configurations were considered for configuration interactions (CI).

## Results and Discussion

**Absorption Spectra in Toluene.** Figure 2 shows the absorption spectra of compounds **1** and **2** in toluene. The absorption maximum of compound **2** appears at around 333 nm. On

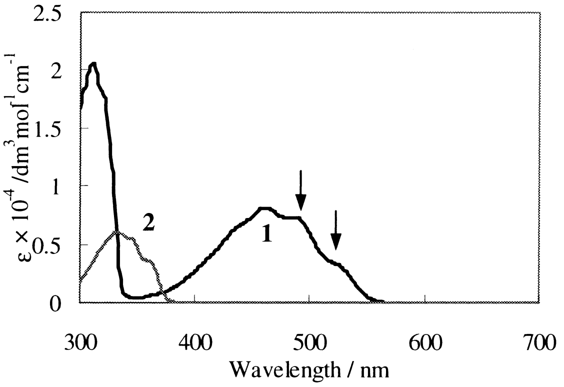

Fig. 2. Absorption spectra of **1** and **2** in $10^{-4}$ M toluene solutions.

the other hand, the maximum for compound **1** appears at a longer wavelength, about 460 nm. The absorption spectrum of **1** is characterized by several absorption shoulders (indicated by arrows) in the longer wavelength region and the maximum peak and the two shoulders are equally spaced with an interval of about 1300 cm$^{-1}$.

In order to clarify this spectral shift in more detail, a semiempirical molecular orbital (MO) calculation was performed for them. The results are summarized in Table 1 and the direction of the dipole moments as well as the transition moments ($\mu$) for **1** and **2** are shown in Fig. 3. The absorption band of **1** in the experiment is located at a much longer wavelength than that of the calculated values, while that of **2** appears at approximately the same wavelength both in calculations and in experiments. Although the solvent parameter of toluene was considered in this calculation, the result was almost the same as that in the free space. Since the magnitude of the dipole moment of **1** (7.6 D) is more than three-times larger than that of **2** (2.3 D), it would be expected that the large dipole moment would enhance the electron delocalization to shift the absorption band toward longer wavelengths. This is consistent with the HOMO (highest occupied molecular orbital)/LUMO (lowest unoccupied molecular orbital) diagrams for compound **1** and **2**, as shown in Fig. 4, where only pyrroloquinoxaline skeletons are illustrated for simplicity. In the HOMO state (ground state), the electron of **1** is mainly distributed over the 1,3-positions of the pyrrole moiety. On the other hand, the electron is uniquely located at the 2-position, while the nitrogen on the pyrrole ring is positively charged in the LUMO (excited state). The present chromophore forms a push-pull system composed of the electron-donating pyrrole nitrogen (i.e. a lone pair of electrons) to the electron-withdrawing part of methoxycarbonyl group, which is responsible for an electron-transfer from donor to the acceptor, as illustrated in Fig. 5. Consequently, this push-pull interaction leads to a bathochromic shift in the absorption spectrum. On the other hand, the electron of **2** is not distributed in the pyrrole moiety, in either the ground or the excited states, as extensively as that of **1**. This result indicates that the lone pair of electrons on the nitrogen of the pyrrole ring are completely involved in the aromatic 6 π systems, and no net charge is observed on the nitrogen in both the HOMO and the LUMO states. Since the effect of the push-pull system would not be expected for compound **2**, it is reasonable that **2** is colorless. Although it is evident that the contribution of the charge-transfer state of **1** shifts the spectra to the orange region in solution, **1** has a red color in the solid state. In order not only to investigate other reasons for this large bathochromic shift from orange in solution to red in the solid state, but also to confirm the polarized structure of **1**, an X-ray single crystal analysis was performed.

**X-ray Single Crystal Analysis of Compound 1.** Figure 6 shows projections of the molecular packing onto (1) the (*b*,*c*) plane and (2) the (*a*,*b*) plain of **1**. The crystal of **1** belongs to the polar space group of *P*1; its crystal system is triclinic. Relevant crystallographic data are summarized in Table 2. The typical bond lengths of the pyrrole moiety of **1** are shown in Fig. 7. Since the bond lengths of N1–C2 and C3–C6 are shorter than those of N1–C5 and C4–C8, it is clear that compound **1** takes the polarized form, which should have aromaticity, like the 10 π electron system shown in Fig. 5. The calculated absorption spectrum using the crystal data of compound **1** had a quite similar shape to that in the free space.

Because of the large dipole moment, the two molecules are arranged in a zig-zag fashion, as shown in Fig. 6 (2), so as to reduce the electrostatic energy. Molecules A and A′ belong to the same conformation, while molecules B and B′ belong to the other. Therefore, the crystal packing of **1** shows the now familiar coplanar π–π stacking. Since the overlapping of the π-orbital is increased, the π–π* transition becomes easy. Consequently, it would be expected that the absorption spectrum of **1** would be shifted toward longer wavelengths, compared to that in solution.

**Polarized Reflection Spectra and Crystal Structure of Compound 1.** Figure 8 shows the polarized reflection spectra measured on the (010) plane of a single crystal of **1** by means of a microscope-spectrophotometer. Prominent reflection bands appear around 490, 520, and 555 nm for polarization perpendicular to the *a*-axis. The present reflection maximum is shifted toward longer wavelengths as compared with that of the absorption band in solution by about 60 nm (2508 cm$^{-1}$). On the other hand, the intensities of these bands are greatly diminished for polarization parallel to the *a*-axis. (Monotonous reflection beyond 550 nm for both polarizations is also observed. This is due to reflection from the rear plane of

Table 1. Optimized Geometries and Absorption bands for Compounds **1** and **2**

| | Dipole | Transion | Calculated | | Observed | |
|---|---|---|---|---|---|---|
| Compounds | moment/D | moment/D | $\lambda_{max}$/nm | $f$$^{a)}$ | $\lambda_{max}$/nm | log $\varepsilon$$^{b)}$ |
| **1** | 7.6 | 3.6 | 392 | 0.64 | 460 | 0.81 |
| **2** | 2.3 | 3.4 | 348 | 0.51 | 333 | 0.65 |

a) Oscillator strength. b) Molar extinction coefficient.

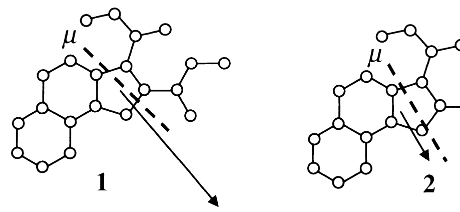

Fig. 3. Direction of dipole moments and transition moments ($\mu$) of **1** and **2**.

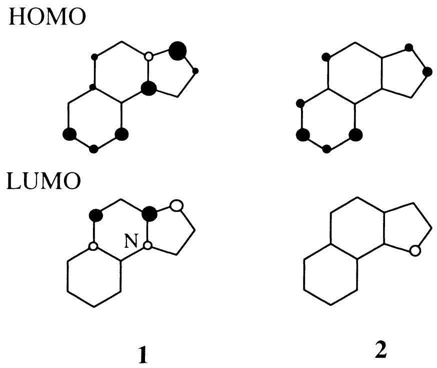

Fig. 4. HOMO and LUMO diagrams for compounds **1** and **2**. The open and closed circles denote the positive and negative signs of the coefficients of the molecular orbitals. The size of each circle is proportional to the MO coefficient.

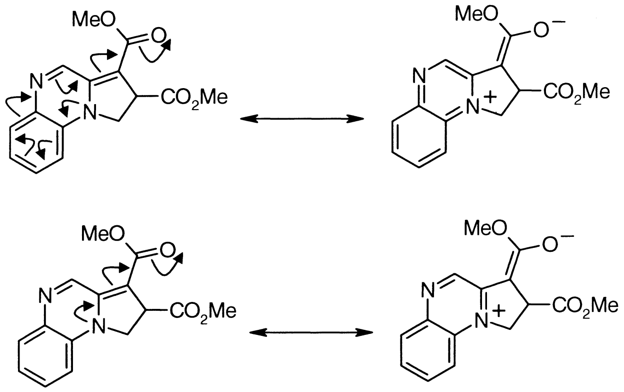

Fig. 5. Two plausible electron flows and resonance structures of compound **1**.

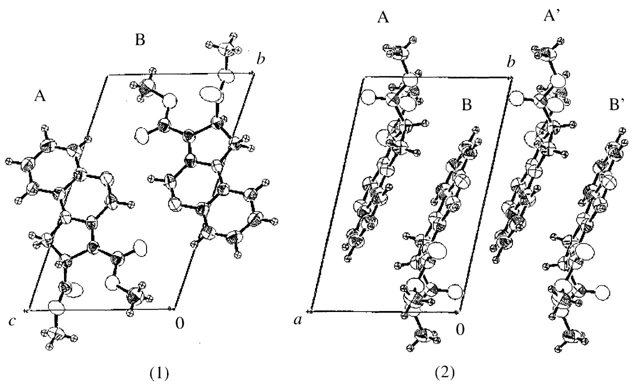

(1) (2)

Fig. 6. Projection of the crystal structures of **1** onto (1) the (*b*, *c*) plane and (2) the (*a*, *b*) plane.

Table 2. Crystallographic Data of **1**

| | **1** |
|---|---|
| Empirical formula | $C_{15}H_{14}N_2O_4$ |
| Fw | 286.29 |
| Color | red |
| Habit | block |
| Crystal system | $P1$(#2) |
| Space group | triclinic |
| $a$/Å | 8.1164 |
| $b$/Å | 12.4175 |
| $c$/Å | 7.9891 |
| $\alpha$/deg | 105.605 |
| $\beta$/deg | 115.067 |
| $\gamma$/deg | 93.710 |
| $V$/Å$^3$ | 687.57 |
| $Z$ | 2 |
| $D_{\mathrm{calc}}$ | 1.383 |
| $R$ | 0.092 |
| $Rw$ | 0.094 |
| $R_1$ | 0.092 |

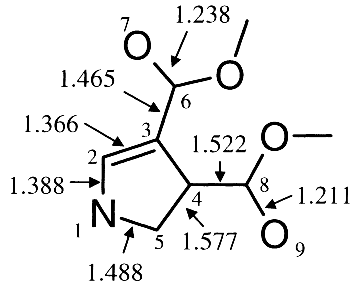

Fig. 7. Typical bond lengths of pyrrole moiety of compound **1**.

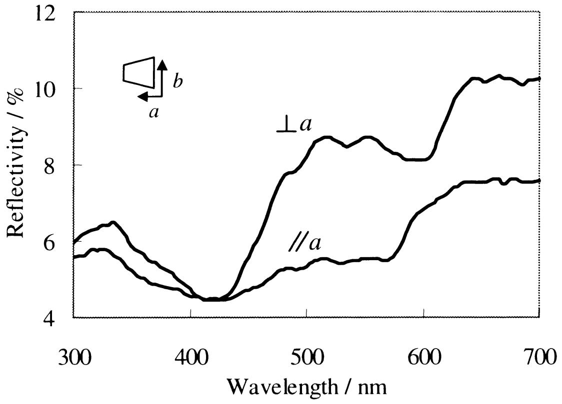

Fig. 8. Polarized reflection spectra of **1** measured on (010) plane.

the single crystal.)

When photoexcitation induces a transition dipole in the molecule, the excited state in the crystals involves wave functions with significant probabilities for the nearest neighbors. Therefore, excitation coupling may well contribute to energy contributions with all of these nearest-neighbor molecules acting in the lattice. This may lead to band splitting of the excited state (Davydov splitting) or a shift in the excited energy level downward (red shift) or upward (blue shift), depending on the relative orientation of the transtion dipoles: "head-to-tail" or "parallel".[15–17]

Concerning the exciton coupling, the present reflection bands are assigned, as follows, by considering the polarization direction as well as the transition moments. Polarization perpendicular to the *a*-axis induces considerable reflection because of the nearly head-to-tail arrangement of the transition dipoles, as shown in Figs. 3 and 6 (1). Likewise, the weak dispersion of polarization parallel to the *a*-axis is due to the small vector component of the transition dipole along the *a*-axis. Based on the above discussion, the bathochromic shift upon crystallization can be attributed to excitonic interactions, in addition to a crystal shift effect.

## Conclusions

The electronic structure of compound **1** was investigated based on the crystal structure and MO calculations. The following conclusions can be drawn from the present investigation:

1. The spectral shift of **1** toward longer wavelengths (460 nm), compared to **2** (333 nm), can be attributed to a push-pull system ranging from the pyrrole nitrogen to the methoxycarbonyl group. On the other hand, the lone pair of electrons on the pyrrole nitrogen of **2** is involved in the aromatic 6π electron system and, hence, its electron donating property is very weak.

2. The absorption band of **1** is shifted toward longer wavelengths by about 60 nm (2508 cm$^{-1}$) upon going from a solution to the solid state. These results cause the unique property of **1**, which is being red in color in the solid state.

This work was supported, in part, by General Sekiyu Research and Development Encouragement and Assistance Foundation. We also acknowledge Prof. J. Mizuguchi for helpful discussions.

## References

1 P. A. Lewis, "Pigment Handbook," John Wiley & Sons, New York (1988).

2 B. L. Kaul, *J. Col. Chem.*, **12**, 349 (1987).

3 G. Graser and E. Hädicke, *Liebigs Ann. Chem.*, **1980**, 1994.

4 Y. Nagao, K. Tsuda, K. Kozawa, and T. Uchida, *Heterocycles*, **54**, 757 (2001).

5 W. Herbst and K. Hunger, "Industrial Organic Pigments," VCH, Weihneim (1997).

6 J. Griffith, "Colour and Constitution of Organic Molecules," Academic Press, New York (1976).

7 D. G. Farnum, *Tetrahderon Lett.*, **29**, 2549 (1974).

8 A. Iqbal, L. Cassar, A. C. Rochat, J. Phenninger, and O. Wallguist, *J. Coat. Technol.*, **60**, 37 (1988).

9 H. Zollinger, "Color Chemistry," VCH Weihneim (1991).

10 J. Mizuguchi, *J. Phys. Chem. A*, **104**, 1817 (2000).

11 J. Mizuguchi, A. C. Rochat, and G. Rihs, *Ber. Bunsenges. Phys. Chem.*, **98**, 19 (1994).

12 M. Ohno, M. Komatsu, H. Miyata, and Y. Ohshiro, *Tetrahedron Lett.*, **32**, 5813 (1991).

13 M. Komatsu, M. Ohno, S. Tsuno, and Y. Ohshiro, *Chem. Lett.*, **1990**, 575.

14 J. J. P. Stewart, "MOPAC Version 2.0," Fujitsu, Tokyo.

15 M. Kasha, "Spectroscopy of the Excited State," Plenum Press, New York (1976).

16 D. P. Craig and S. H. Walmsley, "Excitons in Molecular Crystals," W. A. Benjamin, New York (1968).

17 R. M. Hochstrasser, "Molecular Aspects of Symmetry," W. A. Benjamin, New York (1966).